

# Toughening of Trifunctional Epoxy System. V. Structure–Property Relationships of Neat Resin

R. J. VARLEY,<sup>1</sup> J. H. HODGKIN,<sup>1</sup> G. P. SIMON<sup>2</sup>

CSIRO Molecular Science, Bayview Avenue, Clayton, Victoria 3168, Australia

Department of Materials Engineering, Monash University, Clayton, Victoria 3168, Australia

Received 10 May 1999; accepted 18 May 1999

**ABSTRACT:** This work presents an investigation into the structure–property relationships of a cured highly crosslinked epoxy/amine resin system. The mechanical, physical, and thermal properties of the cured and postcured networks were measured and compared to the chemical structures. Crosslink density was shown to be dependent upon secondary amine conversion and it determined the glass transition temperatures, water uptake, density, toughness, and compressive strength. Other properties such as compressive modulus and yield stress were determined by more short-range molecular motions. Curing at a temperature of 150°C was shown to be the minimum temperature required to “completely” cure the network and achieve optimum mechanical, physical, and thermal properties. © 2000 John Wiley & Sons, Inc. *J Appl Polym Sci* 77: 237–248, 2000

**Key words:** epoxy resin; network structure; thermal, mechanical, and physical properties

## INTRODUCTION

It is well known that cured epoxy resins form highly crosslinked materials that are inherently brittle. The challenge of toughening them has been an active field of research for the past 20 years,<sup>1–3</sup> but a limiting factor has been the lack of understanding of their structure–property relationships. Unfortunately, developing an understanding of structure–property relationships for thermosetting materials is very difficult, which is primarily due to the fact that it is virtually impossible to systematically vary a single parameter without affecting another. Another difficulty is that the cured material becomes completely intractable, rendering many analytical techniques such as gel permeation chromatography (GPC) and high performance liquid chromatography

(HPLC) unusable. In spite of this impediment, many studies have been performed that related the crosslink density of the epoxy resin to material properties such as the glass transition temperature ( $T_g$ ), toughness, modulus, and density and free volume.

Many studies found that increasing the crosslink density of epoxy resin systems caused the  $T_g$  to increase.<sup>4–6</sup> This is because a more tightly crosslinked network requires more energy to enable wholesale cooperative molecular motion at the glass transition point. An equation derived by Fox and Loshaek<sup>7</sup> highlights this dependency of the crosslink density and is as follows:

$$T_g = T_g^\infty + \frac{K_R}{M_c} \quad (1)$$

where the  $T_g^\infty$  is the  $T_g$  of the uncrosslinked polymer of infinite molecular weight,  $K_R$  is a material constant, and  $M_c$  is the molecular weight between two crosslinks. Another relationship between the

---

Correspondence to: R. P. Varley.

*Journal of Applied Polymer Science*, Vol. 77, 237–248 (2000)  
© 2000 John Wiley & Sons, Inc.

$T_g$  and crosslink density was proposed by Nielson<sup>8</sup> from an average of many results published in the literature:

$$T_g - T_{g0} = \frac{3.9 \times 10^4}{M_c} \quad (2)$$

where  $T_{g0}$  is the glass transition temperature of the uncrosslinked polymer and  $M_c$  is the molecular weight between crosslinks (the inverse of the crosslink density).

The literature has generally shown that decreasing the crosslink density causes toughness to increase because of the formation of a looser, more mobile network that is able to absorb energy more efficiently than a highly crosslinked network.<sup>9-11</sup> As early as 1965, Broutman and McGarry<sup>12</sup> observed an increase in toughness with a decrease in crosslink density while using both epoxy and polyester resin systems. Several different means have since been used to vary the crosslink density to investigate the subsequent effect on toughness. The methods have generally involved varying the epoxy/amine stoichiometry<sup>13,14</sup> and systematically increasing the molecular weight between crosslinks of the amine hardener<sup>15,16</sup> or epoxy resin.<sup>17</sup> These results have supported the initial proposition that the toughness of diglycidyl ether of bisphenol A (DGEBA)-based epoxy resin systems increases with decreasing crosslink density.

However, there were other workers who found more complex behavior that appeared to show that the toughness increased with increasing crosslink density. Chang et al.<sup>18</sup> observed an increase in toughness with increasing crosslink density that was attributed to increasing epoxide conversion, and Min et al.<sup>19</sup> also observed an increase in toughness with increasing cure temperature (i.e., crosslink density). These studies highlighted the fact that the reaction must be taken to completion because of the deleterious effects of unreacted functional groups on the mechanical properties of a material. Bell<sup>13</sup> demonstrated an increase in toughness with decreasing crosslink density but also found in the same work that at very high  $M_c$  (low crosslink density) the toughness decreased sharply. This was explained in terms of the structural weaknesses of the network caused by the presence of unreacted amines.

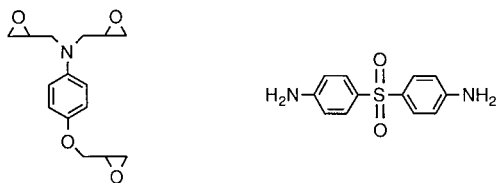
The published literature concerning the effect of increasing crosslink density on the modulus of an epoxy/amine network also contains conflicting

results. Some studies reported that the modulus increases,<sup>20</sup> decreases,<sup>21</sup> or is unaffected by crosslink density.<sup>8</sup> This is because the modulus is more dependent upon small strain properties, such as short-range cooperative localized motion, and not on long-range motions, such as the network crosslinks. The modulus of a material would therefore be expected to be very sensitive to changes in density, free volume, and van der Waals forces. Fischer<sup>22</sup> clearly showed that an apparent increase in modulus with increasing crosslink density was in reality the result of an increase in density of the epoxy/amine network. The rubbery modulus of thermosets, however, was shown to be strongly dependent upon the crosslink density and in fact can be calculated from the rubbery modulus using the following equation:

$$M_c = \frac{\phi \rho R T}{G} \quad (3)$$

where  $\phi$  is the front factor,  $\rho$  is the density,  $R$  is the real gas constant,  $T$  is the absolute temperature, and  $G$  is the equilibrium modulus in the rubbery phase.

Although one may intuitively think that increasing the crosslinking density would result in an increase in density or a decrease in free volume, it was actually reported widely in the literature (primarily for bifunctional DGEBA-based epoxy resins systems) that the reverse is often the case.<sup>19,23-26</sup> This phenomenon was reported by Morgan et al.<sup>4</sup> as being due to the decrease in packing efficiency with increasing crosslink density. Gupta and Brahatheeswaran<sup>26</sup> observed this for a DGEBA/*m*-phenylene diamine (mPDA) system and also explained it in terms of the varying efficiencies of molecular packing at different temperatures. They found that above the  $T_g$  there is a high degree of packing at high crosslink densities, but as the temperature decreases the constraints imposed by the crosslinks cause the rate of contraction to be slower for materials with a high crosslink density than for materials with lower crosslink densities. This causes the network to have a higher free volume and lower density in the glassy state for the more highly crosslinked materials. Experimental results supporting this proposition were also from wide angle X-ray studies by Kumar and Adams.<sup>27</sup> They showed that the average intermolecular distance was the largest in the most highly crosslinked samples. Venditti



Tris glycidyl *p*-amino phenol (TGAP)      Diamino diphenyl sulphone (DDS)

**Figure 1** The chemical structures of the materials used here.

et al.<sup>28</sup> monitored the change in density and free volume with increasing cure conversion (as determined by  $T_g$ ) using a bifunctional epoxy system and found that the density increased rapidly until vitrification after which it decreased with a further reaction in the glassy state. These results were correlated with similar results obtained from positron annihilation lifetime studies that showed that the free volume decreased then increased after vitrification.

This article is the fifth<sup>29–32</sup> in a series of studies relating to the toughening of a trifunctional epoxy resin with a thermoplastic modifier. In this study the structure–property relationships of the neat resin system after cure and postcure were investigated using near IR (NIR) spectroscopy, dynamic mechanical thermal analysis (DMTA), and differential scanning calorimetry (DSC). Physical properties such as water uptake, free volume, and density were also determined, along with mechanical properties such as toughness, compressive modulus, yield stress, and compressive strength.

## EXPERIMENTAL

### Sample Preparation

The epoxy resin used in this study was triglycidyl *p*-aminophenol (TGAP, Ciba–Geigy), a trifunctional, low viscosity, amber liquid sold as Araldite MY0510 and containing 9.41 mmol of epoxide groups per gram of resin. The curing agent or hardener used in all cases was 4,4'-diaminodiphenyl sulfone (DDS, Ciba–Geigy), a pale pink powder sold as Araldite HT976. The epoxy resins and curing agent were used without any further purification and their chemical structures are shown in Figure 1. A slightly off stoichiometric formulation of TGAP/DDS (1:0.9) of epoxide to amino groups, was used for all studies. Neat resin mix-

tures containing TGAP and DDS only were prepared by placing the TGAP and DDS into a round bottom flask and mixing them together on a rotary evaporator under a vacuum at 130°C, using a silicone oil bath for no longer than 30 min. Mixing was continued until the DDS had completely dissolved into the TGAP and was free of bubbles. The resins were then poured into the relevant mold and cured in an oven at temperatures ranging from 100 to 180°C at 10°C intervals for 16 h. For each cure temperature the samples were also postcured at 205°C for 2 h. This meant that there were “cured” and “postcured” samples available for study at each cure temperature.

### DMTA

The  $T_g$  values were obtained from a Polymer Laboratories Mark II DMTA analyzer by clamping a rectangular bar with dimensions of 10 × 1.6 × 45 mm into the dual cantilever bending mode with a 5mm free length frame. The strain amplitude was set at 4 μm and the oscillating frequency used was 1 Hz as the temperature was scanned from 50 to 300°C at a constant heating rate of 2°C/min. The  $T_g$  values were chosen from the peaks in the tan δ spectrum and used consistently as such throughout the work. The low temperature β relaxations were determined using the same method while scanning from –100 to 50°C.

### DSC

A Mettler TA4000 heat flux DSC calorimeter was used to measure the  $T_g$  and cure conversion by placing a sample of between 5 and 10 mg into a 40-μL sealed aluminum crucible into the DSC oven and then performing a dynamic temperature scan from 50 to 300°C at a rate of 10°C/min under a constant flow of N<sub>2</sub>. The  $T_g$  was taken from the midpoint of the endotherm while the conversion was calculated using the following equation:

$$\alpha = 1 - \left( \frac{\Delta H_{\text{residual}}}{\Delta H_{\text{total}}} \right) \quad (4)$$

where  $\Delta H_{\text{total}}$  was 684.0 kJ/mol,  $\Delta H_{\text{residual}}$  is the heat output at time  $t$ , and  $\alpha$  is the fractional conversion.

### Determination of Density

Densities were measured using a Micromeritics pycnometer. Approximately 4 g of resin known to four decimal places was sealed in the pressure

chamber prior to measurement. The pressure that the chamber reached during the fill and purge cycle was approximately 17.5 psi. The measured density was an average of 10 separate measurements.

### Determination of Water Uptake

Water uptake was measured gravimetrically by drying samples in a circulating oven for 2 days to remove any residual moisture prior to testing. Five replicates of each sample ( $10 \times 45 \times 1.6$  mm dimensions) were immersed in water at  $80^\circ\text{C}$  for a total of 14 days and the water uptake was measured by removing the samples at different times, drying them with tissue paper, and then weighing them. This was done after 1, 2, 3, 4, 7, 9, 11, and 14 days of immersion.

### NIR Spectroscopy

NIR spectroscopy was performed on an Alpha Centauri FTIR spectrophotometer (Mattson Instruments) in the NIR mode. Spectra were recorded between  $9000$  and  $4000\text{ cm}^{-1}$  using 32 scans at a resolution of  $8\text{ cm}^{-1}$ . The theory and background to quantifying the epoxide and secondary amine cure conversions from the NIR spectra is described in a previous publication.<sup>29</sup> The difference in the analysis performed here was that the average value of the molar absorptivities calculated for the epoxide and secondary amine groups at  $5881$  and  $6577\text{--}6692\text{ cm}^{-1}$ , respectively, were used. These two peaks were then used to calculate the epoxide and secondary amine conversions after cure and postcure.

To measure the amount of side reactions occurring during cure or postcure, the following equation was used:

$$\alpha_{\text{epoxy}} = \frac{\alpha_{\text{NH}} + 1}{2} \quad (5)$$

where  $\alpha_{\text{epoxy}}$  and  $\alpha_{\text{NH}}$  are the fractional conversions of the epoxide and secondary amines, respectively. This equation assumes that only epoxy/amine addition takes place, so that it can be used to determine a theoretical or "calculated" epoxide conversion from the experimentally determined secondary amine conversions. Any deviation of the experimental epoxide conversion from the calculated epoxide conversion would indicate the occurrence of side reactions.

### Measurement of Fracture Toughness

Fracture toughness testing was carried out using the compact tension method according to ASTM E-394-81 using an Instron 4486 universal tester. Prior to testing, the exact dimensions were measured and the specimens were precracked by inserting a thin razor blade into the machined notch and impacting with a hammer to give a natural crack. In order to prevent crack blunting, a fresh razor blade was used for each specimen. The specimens were then placed into a jig and tested at a crosshead speed of  $1.3\text{ mm/min}$ . After fracture, the exact crack length was measured from the fracture surfaces using an optical microscope fitted with a ruler. The fracture toughness at crack initiation, in terms of the critical stress intensity factor,  $K_{\text{IC}}$ , was calculated according to the following equation:

$$K_{\text{IC}} = \frac{PY}{BW^{1/2}} \quad (6)$$

where  $P$  is the maximum load obtained from the fracture load-deflection curve,  $B$  and  $W$  are the thickness and width of the specimen, respectively, and  $Y$  is expressed as follows:

$$Y = f(R) = \frac{(2 + R)(0.886 + 4.64R - 13.32R^2 + 14.72R^3 - 5.6R^4)}{(1 - R)^{3/2}} \quad (7)$$

where  $R = a/W$  and  $a$  is the crack length. A minimum of five specimens were used to determine the final  $K_{\text{IC}}$  for each test.

### Measurement of Compressive Properties

Compressive tests were also performed using the Instron 4486 universal tester according to ASTM D695-80. Prisms of  $40 \times 10 \times 10$  mm dimensions were machined and placed between horizontal platens with the crosshead speed in each case being  $1.3\text{ mm/min}$  in the downward direction. The compressive modulus, yield stress, and compressive strength were all determined from this test using a minimum of six samples.

## RESULTS AND DISCUSSION

### NIR Spectroscopy

A selection of NIR spectra of the cured TGAP/DDS resin is shown in Figure 2. The decrease in



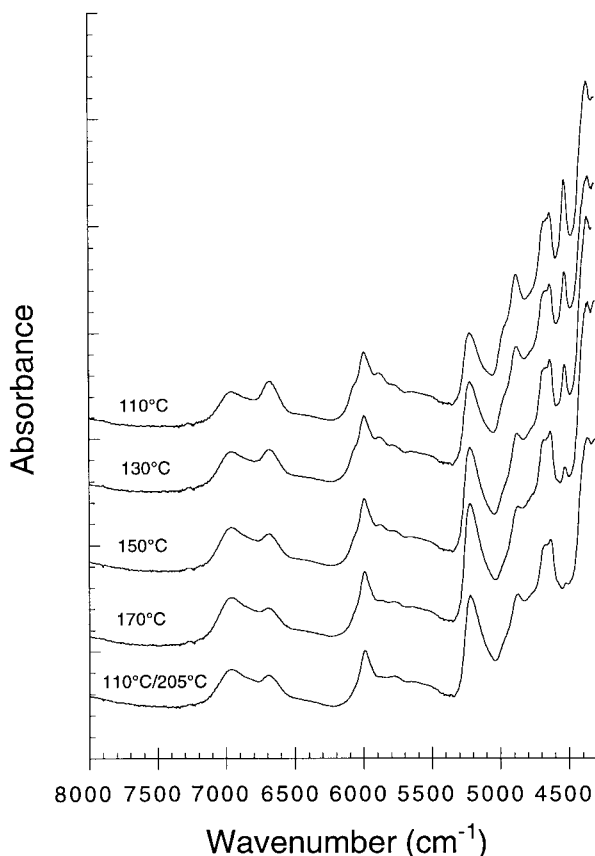


**Figure 2** The near IR spectra of the samples cured at 110, 130, 150, and 170°C. A sample cured at 110°C then postcured at 205°C is also shown.

the size of the epoxide and secondary amine peaks is apparent with increasing cure temperature. However, it can also be seen that after postcure the epoxide groups are virtually eliminated while the secondary amine peaks are not. This immediately suggests that side reactions are occurring. The epoxide and secondary amine cure conversions were plotted versus cure temperature after cure and postcure and are shown in Figure 3. After cure, it is clear that the epoxide conversions increased in a fairly linear fashion with increasing cure temperature. The secondary amine conversions increased in a similar fashion, although from a cure temperature of 150°C onward, further increases in secondary amine conversion were very limited. During postcure the secondary amine conversion increased significantly, particularly at a low cure temperature, but as the cure temperature increased the increase became smaller. In fact, from a cure temperature of 150°C onward there was no further increase in secondary amine conversion as a result of postcure. This

illustrated the fact that although there may have been reactive species present, they were not necessarily able to react if they were sufficiently spatially separated from the epoxide groups in the vitrified network. Conversely, the epoxide conversions after postcure all increased to virtually 100%, regardless of cure temperature. This clearly demonstrated how cure temperature can affect the network structure by controlling the amount of reactive species remaining after cure or postcure. Also shown in Figure 3 is the epoxide conversions of the cured and postcured samples measured from a DSC rescan, which compared very well with the epoxide conversions determined from the NIR spectroscopy.

The results obtained from the cured and postcured networks highlight the differences in reactivity between reactions that occur prior to and after vitrification. Once a material has vitrified, postcuring alone does not necessarily allow all of the further reactions to occur, because of the entrapment of the reactive species in the rigid 3-dimensional network. The decreasing amount of secondary amine reaction occurring with increasing cure temperature during postcure illustrates this clearly. The fact that the epoxide conversion was still able to be completely reacted showed however that amine groups were not a necessary requirement for epoxide groups to be consumed. This suggests that side reactions such as etherification, which may occur through either

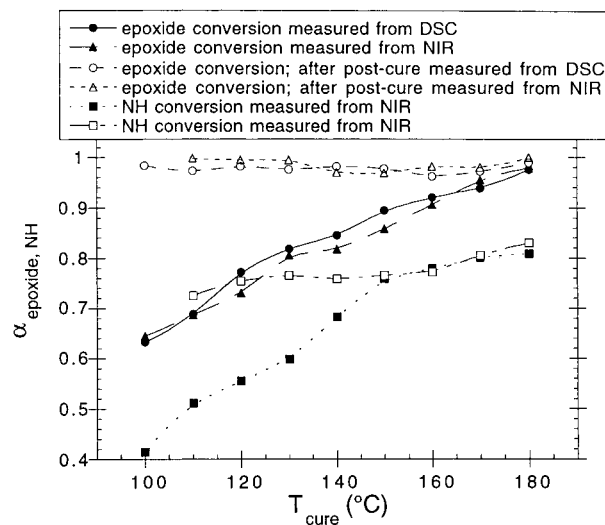


**Figure 3** The plot of the fractional epoxide conversion, measured from DSC and NIR, and secondary amine conversion versus cure temperature after cure and postcure.

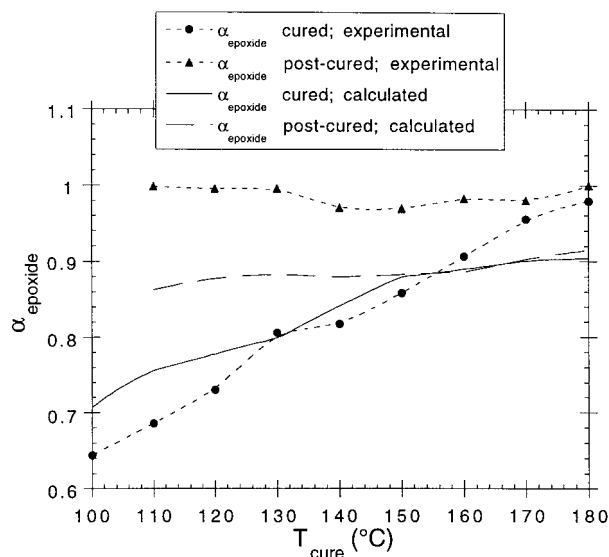


**Figure 4** The plot of the calculated and experimental epoxide conversions versus cure temperature after cure and postcure.

crosslinking or internal cyclization, are taking place.

The amount of etherification occurring in the TGAP/DDS reaction was measured by comparing the experimental epoxide conversion with the calculated epoxide conversion as determined using eq. (5) and the experimental secondary amine conversion. The plot in Figure 4 shows that there are significant differences in the experimental and calculated epoxide conversions after cure and postcure. The experimental data for the cured samples predicted the occurrence of side reactions at cure temperatures of 160°C and above when the calculated epoxide conversion fell below the experimental epoxide conversion. During postcure the etherification became the dominant reaction that was independent of cure temperature, as Figure 4 shows.

From these results the amount of reaction that occurred via secondary amine addition and etherification during cure and postcure was calculated and is shown in Table I. These results indicated that etherification did not start to occur in significant amounts until the cure temperature was 160°C but increased modestly with increasing cure temperature. During postcure, however, it was clear that for low cure temperatures the etherification and secondary amine addition competed equally but as the cure temperature increased, etherification began to dominate until at 150°C virtually all of the reaction taking place

was etherification. Table I also shows, as expected, that the amount of reaction occurring during postcure was far less than that occurring during cure.

## DMTA

Figure 5 shows the  $\tan \delta$  spectra obtained from the dynamic rescan of the cured resin for all of the cured and postcured samples. At lower cure temperatures they displayed two transitions, of which the first (at lower temperatures) increased with increasing cure temperature but gradually decreased in intensity until it was no longer visible. The size of the second transition (at higher temperatures) remained stable, but it also increased with increasing cure temperature, although far more modestly than the first transition. These two transitions are a result of different  $T_g$  values associated with the cured network. The  $T_g$  at the lowest temperature is referred to as  $T_g$ , and this is the  $T_g$  associated with a thermosetting system usually found approximately 10–30°C above the cure temperature. The second transition is denoted  ${}^uT_g$  and corresponds to the maximum  $T_g$  possible for the TGAP/DDS at a particular cure temperature. The appearance of the two transitions, while not common, was reported previously for epoxy resins possessing high functionality. This was observed for a tetrafunctional tetraglycidyl diamine diphenylmethane (TGDDM) DDS resin system by Keenan et al.<sup>33</sup> at lower levels of DDS and was attributed to further curing of unreacted species in the rubbery state. Senich et al.<sup>34</sup> observed this phenomenon for a TGDDM/DDS system and attributed the decrease in size of the  ${}^aT_g$  peak to

**Table I** Secondary Amine ( $\alpha_{\text{NH}}$ ) and Etherification ( $\alpha_{\text{ether}}$ ) Conversion after Cure and Postcure

$T_{\text{cure}}$ (°C)	$\alpha_{\text{NH}}$ after Cure	$\alpha_{\text{ether}}$ after Cure	Further $\alpha_{\text{NH}}$ during Postcure	Further $\alpha_{\text{ether}}$ during Postcure
110	0.51	0.00	0.21	0.27
120	0.56	0.00	0.20	0.24
130	0.60	0.00	0.17	0.22
140	0.68	0.00	0.08	0.18
150	0.76	0.00	0.01	0.17
160	0.78	0.03	0.00	0.19
170	0.80	0.11	0.01	0.15
180	0.81	0.15	0.02	0.17

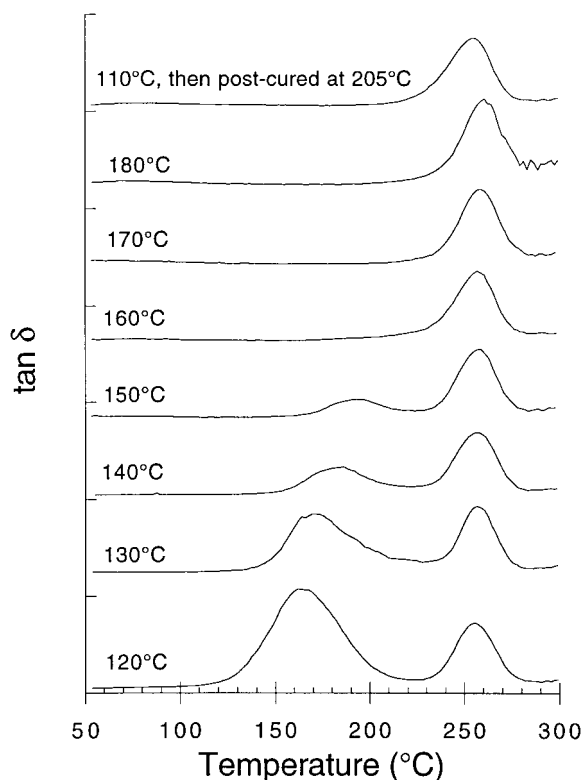


**Figure 5** The  $\tan \delta$  spectra of dynamic rescans after curing at 120, 130, 140, 150, 160, 170, and 180°C. Also shown is the  $\tan \delta$  spectra after curing at 110°C followed by postcuring at 205°C.

the coherence of the network and the decreasing number of reactive sites available with increasing cure conversion. Kim et al.<sup>35</sup> also observed this and explained it in terms of a two phase system containing a continuous crosslinked epoxy phase (the high temperature  $\tan \delta$  peak) and an epoxy oligomeric phase (the low temperature  $\tan \delta$  peak). The latter is converted into the former during cure to form a homogeneous epoxy network resulting in a single  $\tan \delta$  peak corresponding to  ${}^uT_g$ . Regardless of the explanation, the disappearance of the  ${}^\alpha T_g$  peaks effectively means that curing TGAP/DDS at 160°C can produce a material with a  $T_g$  of around 260°C. The NIR studies correlated well with this phenomena in that, at this cure temperature, the secondary amine conversion ceased to increase linearly and showed no further increase with postcure. This confirms that the decrease in intensity of the  $\tan \delta$  peaks was a result of the decreasing number of reactive sites that are able to react.

Figures 6 and 7 compare the changes in  ${}^\alpha T_g$  and  ${}^uT_g$  with secondary amine conversion that

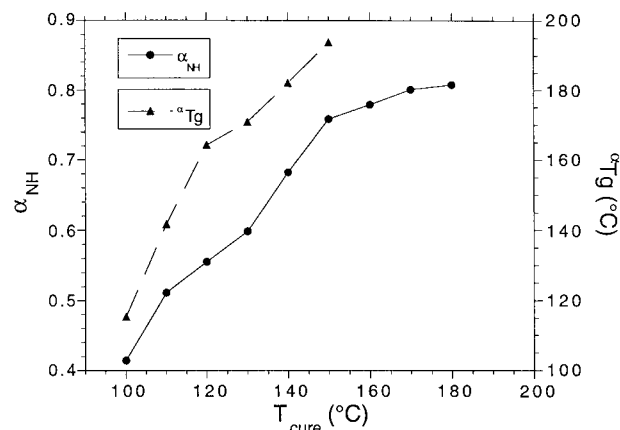


**Figure 6** The plot of secondary amine conversion and  ${}^\alpha T_g$  versus cure temperature.

shows that there is a direct relationship between the  $T_g$  values and the network structure. This clearly demonstrated how increasing secondary amine conversion (crosslinking) increased the thermal properties of the developing network. The much larger increase in  ${}^\alpha T_g$  compared to  ${}^uT_g$  over the same cure temperatures reflects the large differences in the changes in crosslink density of the oligomeric (or reactive) and continuous crosslinked phase.

Obviously, after postcure only the  ${}^uT_g$  transition was observed, and it was found to be very similar to the  ${}^uT_g$  obtained after cure as shown in Figure 8. The similarity between the two  ${}^uT_g$  values indicates that the main effect of postcure is to remove the regions of lower crosslink density (oligomeric phase) by enabling the cure reaction to go to completion, thus producing a network with a

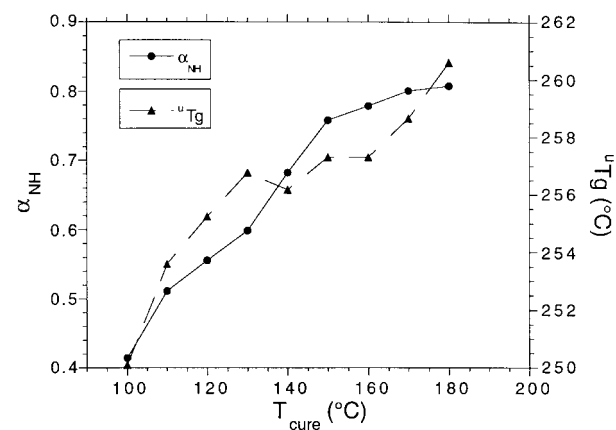


**Figure 7** The plot of secondary amine conversion and  ${}^uT_g$  versus cure temperature.

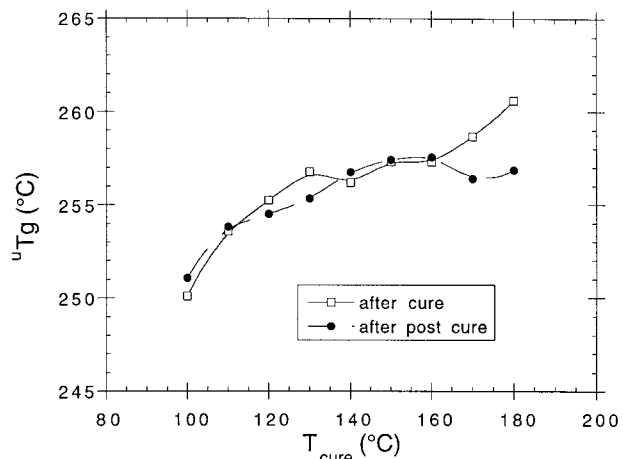


**Figure 8** A comparison of  $^uT_g$  after cure and postcure plotted versus cure temperature.

homogeneous crosslink density. Postcuring increased the crosslink density by allowing the unreacted groups at a lower crosslink density to be consumed, thus incorporating them evenly into the network.

### Water Uptake

The absorption of water by epoxy resins is well known to adversely affect the mechanical properties of a cured epoxy resin. Morgan et al.<sup>36</sup> showed for a TGDDM/DDS resin system the properties such as tensile strength, ultimate elongation, and modulus all decreased when 4% (w/w) water was absorbed by the resin. Water uptake measurements can be difficult to interpret because it is understood to be a measure of both the efficiency of the structural packing of the epoxy network (through water molecules occupying the free volume in a network) and the polarity of the network structure (from the ability of the groups to form hydrogen bonds with water).

A typical example of the rates at which the cured TGAP/DDS network absorbed water during immersion at 80°C for 14 days is shown in Figure 9. The water uptake increased rapidly during the early stages, then leveled off, although not completely, even after the 14 days had elapsed. The final percent water uptake results for the cured and postcured samples after 14 days at 80°C are shown in Figure 10, which shows that increasing cure temperature caused a gradual decrease up until 170°C, after which there was a sharp further decrease at 180°C. After postcure, however, the water uptake was far less sensitive to cure

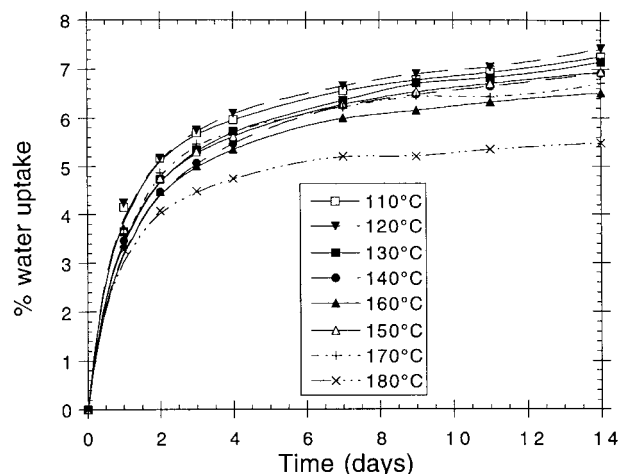


**Figure 9** A plot of the percent water uptakes at varying cure temperatures versus time immersed in water at 80°C.

temperature with the amount of water ingress that occurred being similar to most of the cured samples. For samples reacted at low cure temperatures the moisture absorption was above that of the corresponding postcured samples, probably because of the large amount of unreacted amine groups and the looser, more open nature of the network. As the crosslink density increased and the secondary amine groups were consumed, the moisture ingress eventually fell below that of the postcured sample. Interestingly, this occurred at 150°C, the cure temperature known to first produce a completely formed network. The increasing crosslink density and the increasingly unavailable amine groups caused the moisture absorption to decrease. Clearly, curing at 180°C

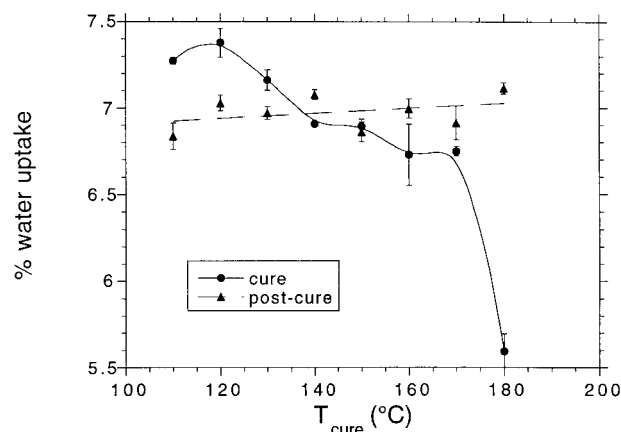


**Figure 10** The final percent water uptake plotted versus cure temperature after cure and postcure.



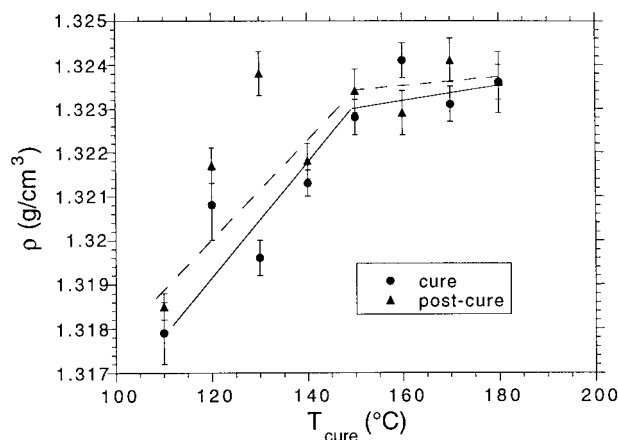


**Figure 11** The density of the cured samples plotted versus cure temperature after (—) cure and (---) post-cure.

caused this effect to be even more pronounced as evidenced by the large further decrease in moisture ingress. The apparent insensitivity of water ingress for the postcured samples may well be a result of an increase in microvoids that, as reported in the literature,<sup>37</sup> can occur as a result of the elimination of unreacted DDS clusters in a TGDDM/DDS resin system.

Water absorption varied between 6.5 and 7.5% for all the samples except for one sample. This value compared well with that of Pethrick et al.,<sup>38</sup> who found that around 7% water was absorbed for the same system after 28 days at 25°C. This amount of water absorption, however, is large in comparison to common DGEBA/DDS systems, which absorb around 2% water under various conditions.<sup>39</sup> A TGDDM/DDS system was found by El-Sa'ad et al.<sup>40</sup> to absorb approximately 5% (w/w) water at 70°C after 28 days, which was more comparable to that of the TGAP/DDS system. Clearly, the higher functionality of the TGDDM/DDS and TGAP/DDS systems indicates that the concentration of hydrophilic groups present in the network have a large bearing on the amount of moisture absorbed by epoxy resins.

### Density

The density of the TGAP/DDS system after cure and postcure was found to increase rapidly with increasing cure temperature as shown in Figure 11. The densities for the cured and postcured samples displayed a large increase until around 150°C, after which no further increase was found. Postcuring the network appeared to increase the

density further, although the increase was marginal. The minimal increase in density at a cure temperature of 150°C and above suggested that in this case there is a direct relationship between crosslink density (or increasing secondary amine conversion) and density. Postcuring was shown to cause a small further increase in density. This result is actually contrary to many studies performed in the literature that showed that increasing crosslink density causes a *decrease* in density. The generally accepted explanation for this, as reported by Gupta and Brahatheeswaran<sup>26</sup> using a DGEBA/mPDA system, is that at high crosslink densities the crosslinking sites prohibit closer packing of rigid molecules. A possible reason for this is that most of these studies were performed using the bifunctional epoxy resin DGEBA. The high degree of linear polymerization of DGEBA that occurs prior to any crosslinking may restrict the closer packing of the network during the crosslinking phase. However, the higher functionality of tri- and tetrafunctional epoxy resins such as TGAP and TGDDM, respectively, form much more branched polymers prior to crosslinking that may have enabled the density to increase with increasing crosslink density. This result is supported by Cizmecioglu et al.<sup>41</sup> who used a tetrafunctional epoxy resin and also found that the density increased with increasing crosslink density.

### Fracture Toughness

The stress intensity factor ( $K_{IC}$ ) or “toughness” of the neat resin samples after cure and postcure was measured using the compact tension method. The fracture toughness values are plotted versus cure temperature in Figure 12 where an increase in toughness is seen for the cured sample with increasing cure temperature up to a cure temperature of 150°C. At higher cure temperatures the  $K_{IC}$  remained fairly constant. Results for the postcured sample results were erratic and showed no real trend with increasing cure temperature but were found to be generally tougher than the non-postcured samples. The fact that curing at 150°C resulted in the optimum fracture toughness clearly highlights again the importance of this cure temperature. The NIR results showed that at this cure temperature the network is “fully cured,” which in this case means that no further epoxy/amine reactions occur. Clearly the lack of toughness at low cure temperatures is a result of the unreacted secondary amines (which are able

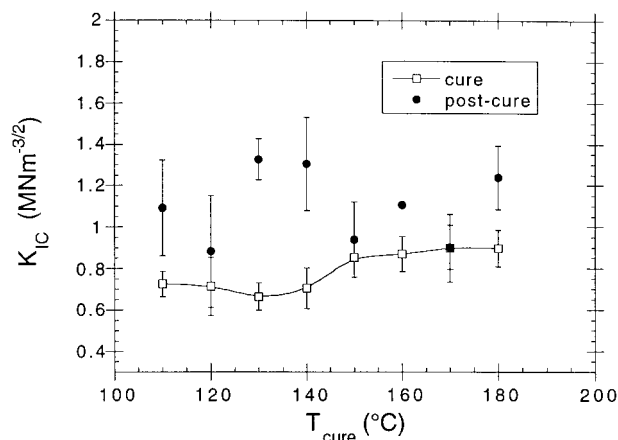


**Figure 12** A plot of the fracture toughness versus cure temperature for the cured and postcured samples versus cure temperature.

to react) producing an incomplete network with structural weaknesses.<sup>13,20</sup>

### Compressive Modulus

The compression modulus was determined from the slope of the linear portion of the stress–strain curve prior to yielding. Figure 13 shows a plot of the moduli obtained at varying cure temperatures after cure and postcure. The modulus was found to decrease with increasing cure temperature after cure but then increased modestly with increasing cure temperature after postcure.

The decrease in modulus arises from the fact that it is not dependent upon long-range microstructural variations such as crosslink density but instead is more dependent upon short-range

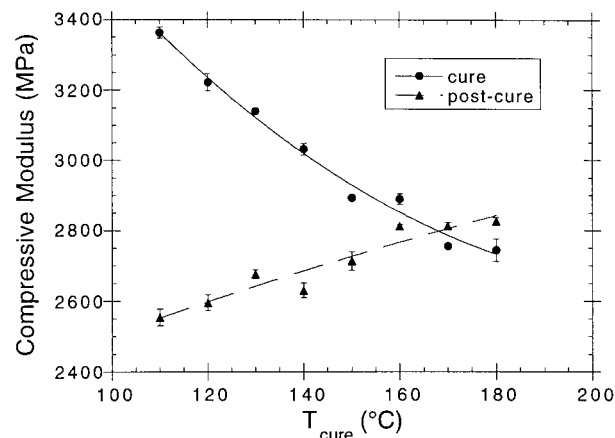


**Figure 13** A plot of the compressive modulus after cure and postcure versus cure temperature.

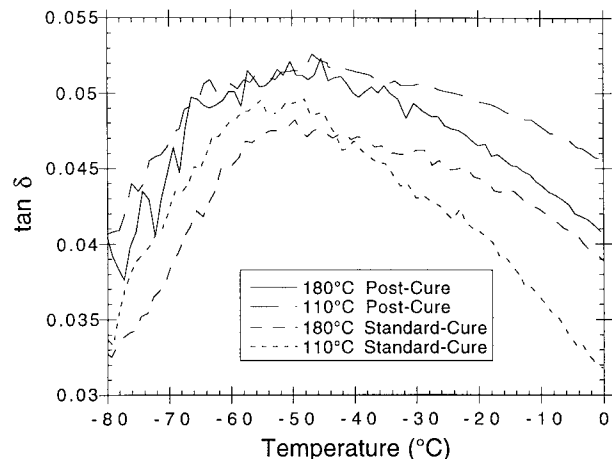


**Figure 14** The dynamic mechanical spectra at 1 Hz showing the  $\beta$  relaxation peaks at cure temperatures of 110 and 180°C after cure and postcure.

motions. Evidence for an increase in the amount of short-range motions occurring is found from the  $\beta$  relaxation spectra obtained from the DMTA. The size and shape of the  $\beta$  relaxations evident in the  $\tan \delta$  spectra reflected the amount of short-range motions occurring. The  $\tan \delta$  spectra for the TGAP/DDS resin cured at 110 and 180°C in Figure 14 clearly show the broadening of the peak on the high temperature side for the 180°C cured sample. This suggests therefore that there are more localized motions occurring for the more highly crosslinked sample and in turn explains the decrease in modulus. This was also reported by Heux et al.<sup>42</sup> who used dynamic mechanical analysis and <sup>13</sup>C-NMR to conclude that an additional number of cooperative motions become available from newly formed crosslinks.

However, after postcure the modulus showed markedly different behavior. The postcured modulus was found to be much lower than the corresponding cured samples, although it increased modestly with increasing cure temperature until there was little difference in the modulus after cure or postcure. The large decrease in modulus at a low cure temperature reflects the much larger range of motions available as a result of the increase in crosslink density, which was evident with the very broad  $\beta$  relaxation peak. The subsequent modest increase in modulus with increasing cure temperature may be a result of the modest increase in density, which restricts molecular motion to a given deformation. Clearly the effect of  $\rho$  is small and is masked when structural considerations dominate, but when structural consid-

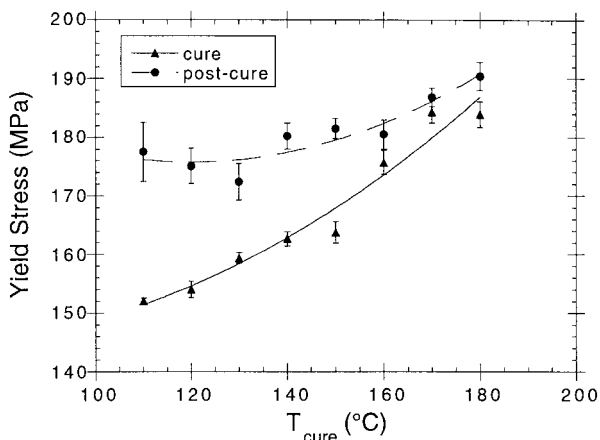


**Figure 15** A plot of the yield stress after cure and postcure versus cure temperature.

erations are equal, as they would be here after postcure, it appears the effect of density on the modulus can be observed.

### Yield Stress and Compressive Strength

The engineering yield stress, which is a small strain property like modulus, is thus not expected to be dependent upon crosslink density. However, Figure 15 shows that it does in fact increase with increasing crosslink density (or cure temperature) for both the cured and postcured samples. The reason for this is more likely to be a result of the increase in density of the network, as opposed to any apparent increase in crosslink density. The significant increase in yield stress with increasing cure temperature after postcure illustrates this well, because it has been shown that density does increase further with cure temperature after postcure.

The compressive strength however is known to be a large strain property that *is* expected to be dependent upon crosslink density.<sup>43</sup> Figure 16 shows that this was indeed the case for the cured TGAP/DDS resin that increased steadily with increasing cure temperature. After postcure the compressive strength increased markedly, but it exhibited little dependence upon cure temperature, again mirroring the observed change in crosslink density.

### SUMMARY

This article presented a detailed investigation of the physical, chemical, and mechanical properties

of the cured TGAP/DDS epoxy resin system. Some of the salient points are listed as follows:

1. At cure temperatures of 150°C and below, the network formed exclusively via epoxy/amine addition reactions while at 160°C and above, etherification began to occur increasingly. After postcure the epoxy/amine addition and etherification reactions competed equally at low cure temperatures, but as the cure temperature increased, etherification became increasingly dominant. The lack of any further increase in secondary amine conversion after postcure showed that, although there were still many remaining reactive secondary amine sites, they were unable to react with epoxide groups because of being immobilized in the rigid network. Thus, curing programs of 150°C or above are required to form a “completely” cured network.
2. The  $T_g$  and  $^*T_g$  both increased with increasing cure temperature and were shown to correlate with the increasing secondary amine conversion. The similarity of the  $^*T_g$  values after cure and postcure indicated that postcuring (or curing at cure temperatures of 150°C or above) marginally increased the crosslink density of the continuous epoxy phase but incorporated the reactive (or “oligomeric,” to use the Kim et al.<sup>35</sup> analogy) species into the continuous epoxy matrix, causing an overall increase in the crosslink density of the network.
3. Optimum fracture properties were only obtained if the reaction was taken to comple-

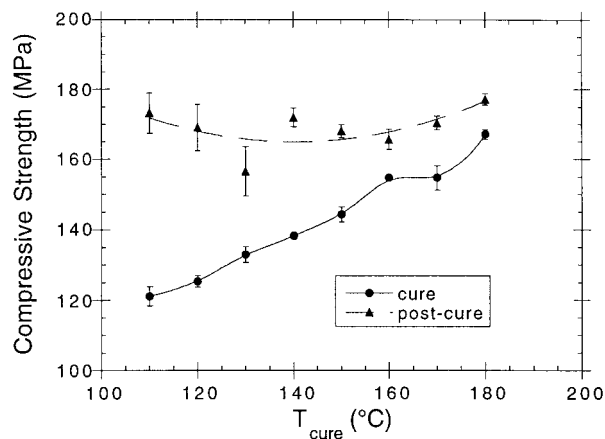


**Figure 16** A plot of the compressive strength after cure and postcure versus cure temperature.

tion. We showed that if the network was not cured at 150°C or above, too many unreacted functional groups remained, which reduced the fracture toughness of the cured network.

4. The modulus was found to be dependent upon short-range molecular motions as characterized by  $\beta$  relaxations. After cure the moduli of the TGAP/DDS network decreased with increasing cure temperature (increasing crosslink density) as a result of the additional number of relaxations available from the newly formed crosslinks. After postcure the modulus increased because of the increasing density.
5. The compressive strength was shown to increase with increasing cure temperature or crosslink density as would be expected because it is a material property known to be dependent upon long-range structural motions. Similarly, the yield stress was also shown to increase with increasing cure temperature, but it was attributed to the increase in density (or decrease in free volume) because it is determined by short-range structural motions.

## REFERENCES

1. Sultan, J. N.; McGarry, F. J. *Polym Eng Sci* 1973, 13, 29.
2. Bucknall, C. B.; Partridge, I. K. *Polymer* 1983, 24, 639.
3. Jackson, M. B.; Edmond, L. N.; Varley, R. J.; Warden, P. G. *J Appl Polym Sci* 1993, 48, 1259.
4. Morgan, R. J.; Kong, F.-M.; Walkup, C. M. *Polymer* 1984, 25, 375.
5. Schroeder, J. A.; Madsen, P. A.; Foister, R. T. *Polymer* 1987, 28, 929.
6. Truong, V.-T.; Truong, Y. B.; Ennis, B. C. *Polym Commun* 1991, 32, 275.
7. Fox, T. G.; Loshaek, S. *J Polym Sci* 1955, 15, 177.
8. Nielson, L. E. *J Macromol Sci Rev Macromol Chem C3* 1969, 1, 69.
9. Vakil, U. M.; Martin, G. C. *J Mater Sci* 1993, 28, 4442.
10. Cook, W. D. *J Appl Polym Sci* 1991, 42, 1259.
11. Levita, G.; DePetris, S.; Marchetti, A.; Lazzeri, A. *J Mater Sci* 1991, 26, 2348.
12. Broutman, L. J.; McGarry, F. J. *J Appl Polym Sci* 1965, 9, 609.
13. Bell, J. P. *J Appl Polym Sci* 1970, 14, 1901.
14. Yamini, S.; Young, R. J. *J Mater Sci* 1979, 14, 1609.
15. Phillips, D. C.; Scott, J. M.; Jones, M. *J Mater Sci* 1978, 13, 311.
16. Scott, J. M.; Wells, G. M.; Phillips, D. C. *J Mater Sci* 1980, 15, 1436.
17. LeMay, J. D. Ph.D. Dissertation, The University of Akron, 1985.
18. Chang, T. D.; Carr, S. H.; Brittain, J. O. *Polym Eng Sci* 1982, 22, 1213.
19. Min, B.-G.; Stachurski, Z. H.; Hodgkin, J. H. *Polymer* 1993, 48, 1303.
20. Chang, T. D.; Brittain, J. O. *Polym Eng Sci* 1982, 22, 1228.
21. Yamini, S.; Young, R. J. *J Mater Sci* 1980, 15, 1814.
22. Fischer, M. *Adv Polym Sci* 1992, 100, 713.
23. Fisch, W.; Hofmann, W.; Schmid, R. *J Appl Polym Sci* 1969, 13, 295.
24. Madsen, P. A.; Foister, R. T. *J Appl Polym Sci* 1989, 37, 1931.
25. Brahatheeswaran, C.; Gupta, V. B. *Polymer* 1993, 34, 289.
26. Gupta, V. B.; Brahatheeswaran, C. *Polymer* 1991, 32, 1875.
27. Kumar, S.; Adams, W. W. *Polymer* 1987, 28, 1497.
28. Venditti, R. A.; Gillham, J. K.; Jean, Y. C.; Lou, Y. *J Appl Polym Sci* 1995, 56, 1207.
29. Varley, R. J.; Heath, G. R.; Hawthorne, D. G.; Hodgkin, J. H.; Simon, G. P. *Polymer* 1995, 36, 1347.
30. Varley, R. J.; Hawthorne, D. G.; Hodgkin, J. H.; Simon, G. P. *J Appl Polym Sci* 1996, 60, 2251.
31. Varley, R. J.; Hawthorne, D. G.; Hodgkin, J. H.; Simon, G. P. *J Polym Sci Part B Polym Phys* 1997, 35, 153.
32. Varley, R. J.; Hodgkin, J. H.; Hawthorne, D. G.; Simon, G. P.; McCulloch, D. *Polymer*, submitted.
33. Keenan, J. D.; Seferis, J. C.; Quinlivan, J. T. *J Appl Polym Sci* 1979, 24, 2375.
34. Senich, G. A.; MacKnight, W. J.; Schnieder, N. S. *Polym Eng Sci* 1979, 19, 313.
35. Kim, B. S.; Chiba, T.; Inoue, T. *Polymer* 1995, 36, 43.
36. Morgan, R. J.; O'Neal, J. E.; Fanter, D. L. *J Mater Sci* 1980, 15, 751.
37. Morgan, R. J.; O'Neal, J. E.; Miller, D. B. *J Mater Sci* 1979, 14, 109.
38. Pethrik, R. A.; Hollins, E. A.; McEwan, I.; McKinnon, A. J.; Hayward, D.; Cannon, L. A.; Jenkins, S. D.; McGrail, P. T. *Macromolecules* 1996, 29, 5208.
39. Aherne, J. P.; Enns, J. B.; Doyle, M. J.; Gillham, J. K. *Org Coatings Plast Chem* 1982, 46, 574.
40. El-Sa'ad, L.; Darby, M. I.; Yates, B. *J Mater Sci* 1990, 25, 3577.
41. Cizmecioglu, M.; Gupta, A.; Fedors, R. F. *J Appl Polym Sci* 1986, 32, 6177.
42. Heux, L.; Halary, J. L.; Laupretre, F.; Monniere, L. *Polymer* 1997, 38, 1767.
43. Madsen, P. A.; Foister, R. T. *J Appl Polym Sci* 1989, 37, 1931.